Proceedings of the 24th European Young Geotechnical Engineers Conference (EYGEC), Durham, UK
Osman, A.S. & Toll, D.G. (Eds.) 2015
ISBN 978-0-9933836-01

3D numerical back-prediction of tunnelling-induced settlements on an existing reinforced concrete building

V. Fargnoli [*1], D. Boldini [1] and A. Amorosi [2]

[1] *University of Bologna, Bologna, Italy*
[2] *Technical University of Bari, Bari, Italy*
[*] *Corresponding Author*

ABSTRACT. This study analyses the evolving response of a 9-storey reinforced concrete building while being undercrossed by an urban metro-line. It refers to the case of the twin-tunnels of the Milan (Italy) metro-line 5, recently built in coarse-grained materials using EPB machines, for which subsidence measurements collected during tunnelling were available. In the finite element study, the soil mechanical behaviour is described by an advanced constitutive model, named Hardening Soil model with small strain stiffness, that, when combined with a proper simulation of the excavation process, proves to realistically reproduce the subsidence profiles observed under free-field conditions. Furthermore, when the numerical model is extended to include the building schematised in a detailed manner, the results are in good agreement with the monitoring data for different stages of the twin-tunnel excavation, indirectly confirming the satisfactory performance of the adopted numerical approach. Conversely, when the building is modelled as an equivalent plate, the results highlight that, in this case, such a schematisation is inadequate to capture the real tunnelling-induced displacement field. The overall behaviour of the system proves to be mainly influenced by the buried portion of the building which plays an essential role in the interaction mechanism, due to its high stiffness.

1 INTRODUCTION

The construction of metro-lines in urban areas is increasing worldwide to develop new facilities for the transportation system. Tunnel excavation works frequently interact with existing structures located nearby to be preserved from any possible induced damage. Thus, a key aspect of these projects is represented by a very careful and detailed assessment of the tunnelling-induced displacement field, which is generally strongly modified by the presence of structures on the ground with respect to free-field conditions.

In several cases, a detailed investigation of the soil-tunnel-structure interaction can only be performed by a 3D numerical approach, which allow to account for any construction scheme and for any kind of structural typology with any relative position with respect to the tunnel. However, the reliability of the numerical approach is strongly affected by different factors, such as the constitutive hypotheses for the soil, the correct simulation of the tunnel excavation sequence and the detail in the structural modelling.

The 3D finite element study presented in this works, performed by the code Plaxis 3D, investigates the interaction process between a reinforced concrete framed building and an urban metro-line. It aims at demonstrating the importance of a proper description of the soil mechanical behaviour, associated to a correct schematisation of the tunnel construction and to an appropriate structural modelling, to realistically simulate the response of the overall system to tunnelling.

The ability of the proposed procedure to effectively capture the soil-tunnel-structure interaction mechanism is validated against the available monitoring settlement measurements from a real case history, i.e. the recent construction of the new Milan (Italy) met-

ro-line 5 (Fargnoli et al. 2013; Fargnoli et al. 2015*a*). This latter diagonally underpasses a multi-storey reinforced concrete framed structure dating back to the end of the 1950s.

2 THE CASE HISTORY

The new metro-line 5 of Milan consists of two twin tunnels, excavated by earth pressure balance (EPB) machines, having a diameter D = 6.7 m, an average distance between their axes of about 15 m and a mean depth of each axis z_0 = 15 m.

During the various stages of the tunnel construction, an extensive geotechnical and structural monitoring campaign was carried out along the line by an accurate levelling survey.

The data presented and discussed in this paper are vertical displacements recorded during the excavation of both tunnels of the metro-line along a free-field ground section and along three sides of a nine-storey reinforced concrete framed structure diagonally undercrossed by the first tunnel (Figure 1).

The 30 m high structure is founded on five strip footings (0.65 m high, indicated as I, II, III, IV and V in Figure 2) located at 4 m below the ground surface; more specifically, the building rests on the foundation beams I, II and III, while the garage zone, situated at the basement floor level along the right longitudinal side of the structure, stands on the other ones (IV and V). Three raft foundations (0.7 m high, indicated as VI, VII and VIII in Figure 2) are located at the same level under the elevator shafts and the stairwell, both resting on the right longitudinal side of the building.

Reinforced-concrete retaining walls (40 cm thick and 3.5 m high) surround the buried portion of the structure along its three sides, with the exception of the right longitudinal side for the access to the garage zone.

Five ground benchmarks were installed on the instrumented ground section S_{35} nearby the building, while several monitoring targets were placed at the base of the building along the longitudinal façades and on its transversal right side (see Figure 1).

At the reference site the soil stratigraphy consists of two gravelly-sand strata (effective friction angle φ' = 33°) at the depths 0-20 m and 25-30 m and of a sandy-silt layer (cohesion c' = 5 kPa and φ' = 26°) identified between 20 m and 25 m. The hydrostatic water level is located at an almost constant depth of about 15 m below the ground surface.

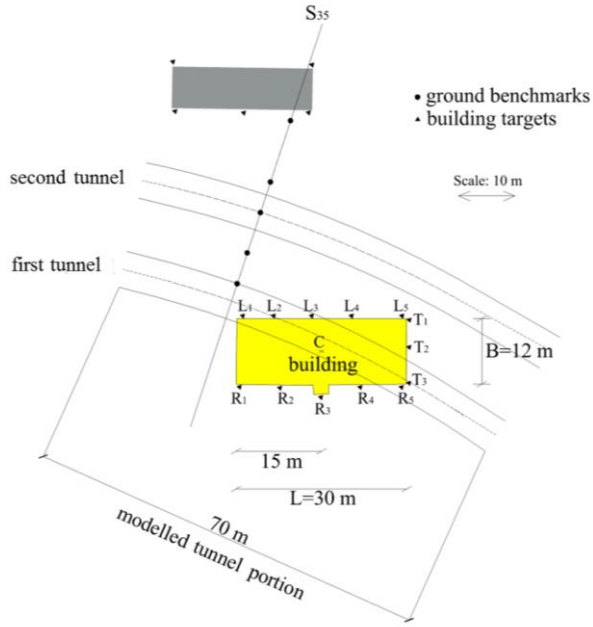

Figure 1. Detail of the examined portion of the route.

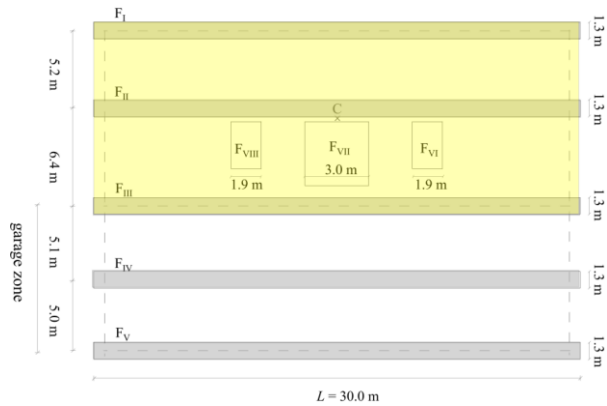

Figure 2. Plan view of the building's foundation system.

The total unit volume weights under saturated conditions, γ, for the gravelly-sand and for the sandy-silt soils are equal to 20 kN/m^3 and 17.5 kN/m^3, respectively.

No geophysical investigations were specifically carried out at the construction site. The one closest to the investigated portion of the metro-line route is a

down-hole test resulting in the small strain shear modulus (G_0) profile with depth shown in Figure 3.

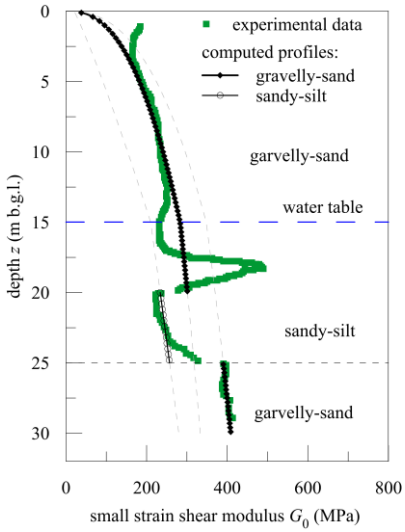

Figure 3. Experimental and computed G_0-z profiles (the soil stratigraphy and the position of the water table are also shown).

3 THE FINITE ELEMENT MODEL

The numerical model (80 m x 100 m x 30 m) set up to simulate the interaction between the twin tunnels of the metro-line 5 and the investigated framed building is shown in Figure 4. The soil profile refers to the subsoil conditions encountered along the segment of the route where the building is located and it was defined according to the *in situ* stratigraphy.

The mechanical behaviour of the soils is described by the Hardening Soil model with small strain stiffness (HSsmall, Benz, 2007). The values of the strength parameters (c′ and φ') and of the total unit volume weighs used in the model were equal to those defined in the previous section, while the variation of the small strain stiffness with depth was obtained by calibrating the parameters G_0^{ref} and m against the down hole experimental results, as shown in Figure 3. The assumed shear stiffness decay curves for the gravelly-sand and sandy-silt layers follow the empirical ones proposed by Vucetic and Dobry (1991) for granular soils (plasticity index I_P = 0) and for low plasticity silts (I_P = 15 %), respectively. As such, the shear strain at which the shear modulus is reduced to about 70% of its initial value (i.e. $\gamma_{0.7}$) was selected with reference to these curves.

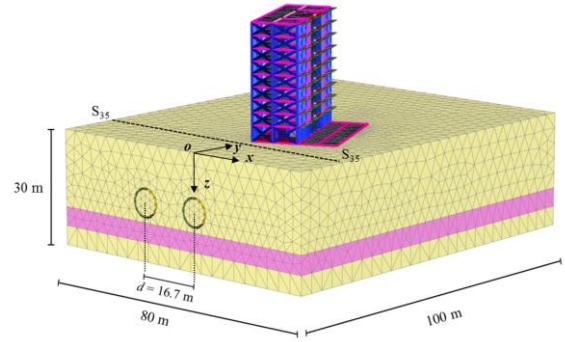

Figure 4. Finite element model and sketch of the mesh

The reference Young's modulus at small strains, $E'_0{}^{ref}$, is related to $G_0{}^{ref}$ by the Poisson's ratio for unloading/reloading, ν_{ur}. This latter was set equal to 0.2 and 0.25 for the gravelly-sand and for the sandy-silt, respectively. The reference unloading/reloading stiffness, $E'_{ur}{}^{ref}$, was assumed equal to 0.24 $E'_0{}^{ref}$ for the gravelly-sand and 0.42 $E'_0{}^{ref}$ for the sandy-silt. These stiffness values correspond to those observed along the decay curves at γ = 0.1%. The other stiffness parameters, $E'_{50}{}^{ref}$ and $E'_{oed}{}^{ref}$, were assumed three times lower than $E'_{ur}{}^{ref}$.

In particular, for the gravelly-sand of the first stratum: m = 0.4, $\gamma_{0.7}$ = 0.0001, $G_0{}^{ref}$ = 250000 kPa, $E'_{50}{}^{ref} = E'_{oed}{}^{ref}$ = 48000 kPa, $E'_{ur}{}^{ref}$ = 144000 kPa; for the sandy-silt layer: m = 0.85, $\gamma_{0.7}$ = 0.0002, $G_0{}^{ref}$ =155000 kPa $E'_{50}{}^{ref} = E'_{oed}{}^{ref}$ = 54250 kPa, $E'_{ur}{}^{ref}$ =162750 kPa; for the gravelly-sand of the third stratum: m = 0.4, $\gamma_{0.7}$ = 0.0001, $G_0{}^{ref}$ = 307000 kPa, $E'_{50}{}^{ref} = E'_{oed}{}^{ref}$ = 58944 kPa, $E'_{ur}{}^{ref}$ = 176832 kPa.

For all soil layers the overconsolidation ratio was fictitiously imposed to be large enough to exclude the activation of the cap yield surface of the constitutive model.

As in the reference case study, the tunnels have a diameter D = 6.7 m and their axes are located at a depth z_0 = 15 m; the axis-to-axis tunnel horizontal distance, d, is equal to 16.7 m.

The excavation of each tunnel was simulated by a step-by-step numerical procedure (Figure 5) consisting of 43 advancements, each having the length of one concrete lining ring (1.4 m), from y = 9.8 m to y = 70 m. The advancement consists in removing a 1.4 m long slice of soil inside the tunnel and impos-

ing dry conditions. The tunnel boundaries were considered as impervious. At each advancement, a pressure is applied at the new tunnel face, corresponding to the estimated total horizontal stress acting at rest $\sigma_{h0}(z)$, which ranges from 106 kPa at the tunnel crown to 185 kPa at the invert for both tunnels.

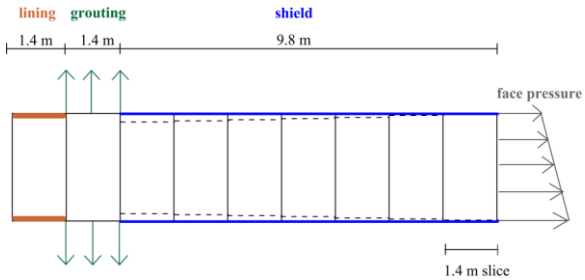

Figure 5. Scheme of EPB tunnelling.

In between the shield tail and the permanent lining, a 1.4 m length of soil is supported by a uniform pressure representing the action of grouting applied to back-fill the lining after the installation. According to the average monitored values (Fargnoli 2015*b*), the grouting pressure was set equal to 150 kPa and 170 kPa for the first and second tunnel, respectively.

The shield (thickness = 0.03 m, unit volume weight = 75 kN/m^3, Poisson's ratio = 0.25 and Young's modulus 210 GPa) and the lining (thickness = 0.3 m, unit volume weight = 25 kN/m^3, Poisson's ratio = 0.15 and Young's modulus 35 GPa) were introduced in the numerical model by plate structural elements with isotropic linear-elastic behaviour.

In order to generate a subsidence volume at the ground surface, a fictitious contraction was applied along the shield, starting from the second slice. Such a contraction is characterised by a constant increment along each slice, aiming at reproducing in a simplified way the shield conical geometry.

The foundations of the building were modelled by 10-node tetrahedral volume elements constituted by a non-porous material, while 3-node line beam elements were used for beams and columns and 6-node triangular plate elements with isotropic behaviour were used for floor slabs, reinforced concrete interior panels, elevator shafts, stairwell and retaining walls.

A linear-elastic constitutive law was adopted for these structural components, whose parameters were selected consistently with the reinforced concrete material properties: unit volume weight γ_c = 24 kN/m^3, Young's modulus E_c = 25 GPa and Poisson's ratio ν_c = 0.2.

The external infill panels of the building were modelled in a simplified way by means of equivalent cross-bracings having a width defined following Mainstone (1971). The cross bracings are 2-node anchor weightless elements characterised by an elasto-plastic constitutive law.

Two additional numerical schemes were also set up adopting different levels of detail in the structural modelling, limiting in this case the analysis to the interaction with the first tunnel of the metro-line.

The building was first limited to its buried portion including the foundation elements and the retaining walls (analysis STR$_w$). In this model, the upper portion of the structure was reduced to equivalent loads applied in correspondence with the columns' head, the stairwell and the elevator shafts. Then, the structure was strongly simplified and schematised as an equivalent plate (L = 30 m and B = 12 m) in terms of stiffness and weight, placed at the foundation level (analysis STR*), according to the approach proposed by Franzius et al. (2006). In this model the retaining walls were also introduced.

4 NUMERICAL RESULTS AND COMPARISON WITH MONITORING DATA

The ability of the numerical approach to back-predict the tunnelling-induced settlements was firstly checked at the transversal ground section S$_{35}$ for the volume loss values observed at the end of the first and the second excavation, equal to $V_L^{(I)}$ = 0.34% and $V_L^{(TOT)}$ = 0.42% respectively. As shown in Figure 6, the computed profiles, Gaussian empirical curves (Peck 1969; New & O'Reilly 1991) and monitoring data are in fair agreement, confirming the capability of the simulation to capture the interaction phenomenon between the twin tunnels. This latter results in an increase in the maximum settlement above the first tunnel axis after the completion of the second excavation and in a non-symmetric final subsidence profile. In particular, the numerical curve obtained after the second tunnel excavation well reproduces the corresponding measurements, irrespectively of the fact that the same comparison was not very satisfactory after the first tunnel excavation, as the settlements

measured in that case at $x \leq 16.7$ m resulted underestimated.

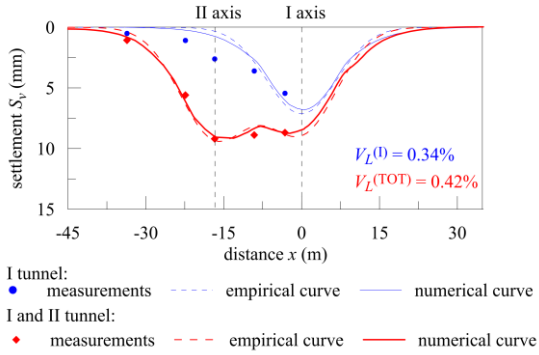

Figure 6. Comparison of computed profiles, Gaussian curves ($K = 0.45$) and measured settlements.

The results of the numerical analysis performed including a detailed structural model (named STR) are shown in Figure 7 (*a-c*) in terms of settlements. They are compared with measurements collected at selected stages of the excavation process along the left and right longitudinal façades of the building and along its transversal side. In particular, reference is made to the observations carried out for a position of the first tunnel face at the middle of the structure (point C in Figure 1) and at the end of the first and the second excavation, respectively. It is possible to observe that the computation provides subsidence profiles along each building façade that well reproduce the measured vertical displacements, accurately predicting the deformative pattern of the building.

The proposed integrated, geotechnical and structural, approach also allows a direct investigation of the structural response, as shown in the example of Figure 8. It illustrates the axial stresses acting within the cross-bracings of the longitudinal left façade, characterised by larger total and differential settlements, when the building experiences a predominantly hogging-type mode of deformation, i.e. when the first tunnel face is located at the middle of the structure. According to the deformative mechanism, the cross bracings subjected to axial tensile stresses, represented by dashed lines in the figure, are located in the upper levels of the structure. The computed values of the tensile strain are always lower than 0.004 % and this is consistent with the absence of damage observed *in situ* on this structure (Boscardin & Cording 1989).

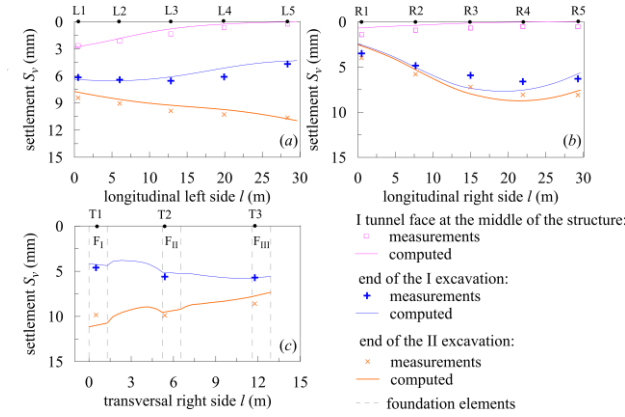

Figure 7. Comparison between measured and computed settlements along the building's façades during tunnelling.

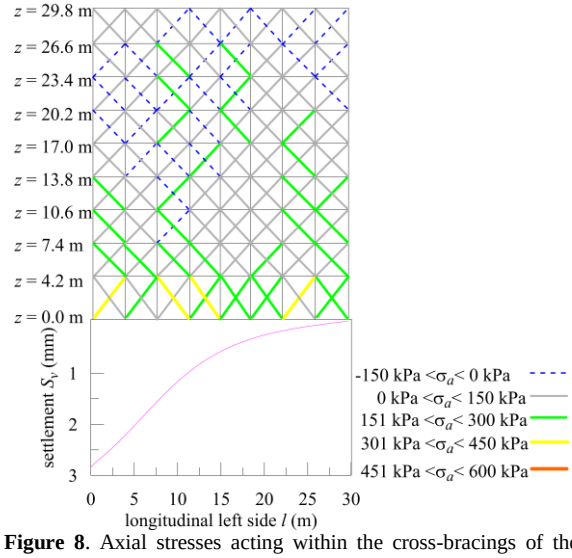

Figure 8. Axial stresses acting within the cross-bracings of the longitudinal left façade of the building.

The numerical results obtained introducing in the finite element model simplified structural schemes are reported in Figure 9 with reference to a specific stage of the tunnelling process, that is the complete excavation of the first tunnel directly underpassing the building. The STR_w displacement curves are very similar to the STR ones, thus indicating that, in this particular case, the buried portion of the structure provides the most relevant contribute to the overall stiffness. The STR^* results are unsatisfactory for this specific framed building as its stiffness results to be largely overestimated. These results are also on the unsafe side as the predicted displacement field appears to be characterised by almost rigid rotations

along each side, without indicating any sagging or hogging deformative modes. As expected, the free-field results, reported for comparison in the same figure, lead in each case to less intense settlements with respect to the interaction analyses and to rather overestimated differential ones.

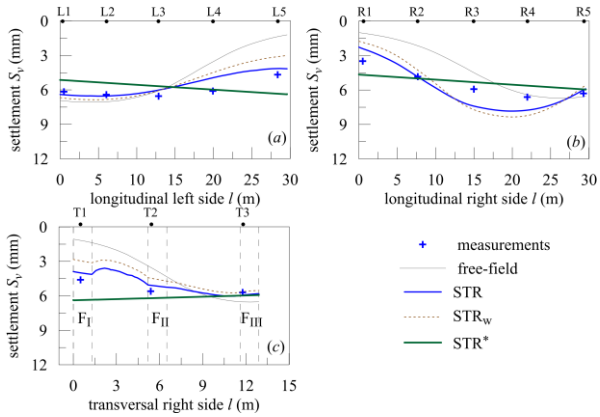

Figure 9. Comparison between measured and computed settlements with different structural models.

5 CONCLUSIONS

This paper is focused on the analysis of the interaction mechanism between a reinforced concrete framed building underpassed and an urban metro-line recently constructed in Milan (Italy).

One element of novelty of this work is the detail adopted in modelling this existing structure influenced by tunnelling activities. In the finite element scheme, the soil mechanical behaviour is described by an advanced model (HSsmall), capable of taking into account the dependency of the soil stiffness on the deformative level and the early accumulation of plastic strains.

When combined with an appropriate schematisation of the excavation process, it is found to be very effective in providing computed subsidence profiles under free-field conditions in accordance with experimental observations for volume loss values typical for EPB tunnelling in coarse-grained soils. Computational results well reproduce the *in situ* observations also when the soil-tunnel-building interaction is modelled considering a detailed structural scheme, being accurate in replicating the modification of the deformative pattern during tunnelling. This result proves the reliability of the proposed approach to capture the essential mechanisms governing the problem. The numerical settlement profiles are found to nicely fit the monitoring data also when the building is reduced only to its buried portion opportunely loaded, highlighting the negligible stiffening role of the above structure in this reference case study.

In contrast, for this particular building and foundation typology, the equivalent plate schematisation involves a large overestimation of the structure's stiffness, resulting in highly inaccurate settlement profiles as compared to that observed *in situ*. This schematisation does not allow to reproduce the real displacement field affecting this building along its longitudinal sides on continuous strip footings, nor along the portions of the structure located between the foundation elements. The equivalent plate model also prevents to capture the sagging and hogging type mechanisms highlighted along each side of the building and the stiffer structural response observed in correspondence with the single foundation beams.

REFERENCES

Benz, T. 2007. Small-strain stiffness of soils and its numerical consequences. *Ph.D. dissertation*, Universität Stuttgart.

Boscardin, M. & Cording, E. 1989. Building response to excavation-induced settlement. *Journal Geotech. Eng*., **115**, (1), 1–21.

Fargnoli, V. Boldini, D. & Amorosi, A. 2013. TBM-tunnelling induced settlements in coarse-grained soils: The case of the new Milan underground line 5. *Tunnelling and Underground Space Technology*, **38**, 336-347.

Fargnoli, V. Gragnano, C.G. Boldini, D. & Amorosi, A. 2015*a*. 3D numerical modelling of soil-structure interaction during EPB tunnelling. *Géotechnique*, **65**, (1), 23-37.

Fargnoli, V. 2015*b*. Soil-structure interaction during tunnelling in urban area: observations and 3D numerical modelling. *Ph.D. dissertation*, University of Bologna.

Franzius, J.N. Potts, D.M. & Burland, J.B. 2006. The response of surface structures to tunnel construction. *Proc. Inst. Civil Engineers-Geotechnical Engineering*, 159, (1): 3-17.

Mainstone, R.J. 1971. On the stiffnesses and strengths of infilles frames. *Proc. Inst. Civil Engineers*, **49,** (2), 59-70.

New, B.M. & O'Reilly, M.P. 1991. Tunnelling induced ground movements; predicting their magnitude and effects. *Proc. 4th Int. Conf. on Ground Movements and Structures*. Cardiff, 671-697.

Peck, R.B. 1969. Deep excavations and tunnelling in soft ground. *Proc. 7th int. conf. on soil mech. and found. eng.* Mexico City, 225-290.

Vucetic, M. & Dobry, R. 1991. Effect of the soil plasticity on cyclic response. *Journal Geotech.Eng.*, **117**, (1), 89-107.